Semarak Engineering Journal

Journal homepage:
https://semarakilmu.my/index.php/sej/index
ISSN: 3036-0145

Ductal Porosity and Thermal Effects on Bile Transport: A Two-Dimensional Peristaltic Flow Model of the Cystic Duct

Devendra Kumar[1], Tanuj Kumar Rawat[2], Mahesh Garvandha[1,*], Sanjeev Kumar[3], Sudhakar Kumar Chaubey[1]

[1] Sciences and Mathematics Unit, Department of Supportive Requirements, University of Technology and Applied Sciences-Shinas, Al Aqr, 77PC324, Oman
[2] GLA University, Greater Noida, India
[3] Dr. Bhimrao Ambedkar University, Agra, India

ARTICLE INFO

Article history:
Received 12 February 2026
Received in revised form 21 March 2026
Accepted 18 April 2026
Available online 20 May 2026

Keywords:
Ductal Porosity, Bile Transport, Thermal Energy, Peristaltic Flow, Cystic Duct

ABSTRACT

Gallstone disease and cystic duct obstruction remain major clinical challenges in hepatobiliary medicine, where altered bile rheology, ductal porosity due to microlithiasis, and heat transfer significantly influence bile transport and stone formation. The present model provides theoretical insight into the combined effects of thermal gradients, porous resistance, and non-Newtonian bile rheology on cystic duct flow under simplified physiological conditions. The model is developed under low Reynolds number and long wavelength assumptions and does not incorporate full three-dimensional anatomical complexities. Governing equations are solved numerically using a finite difference method. Parametric analysis reveals that axial velocity decreases with increasing baffle height and duct porosity but rises with higher Grashof number (buoyancy effects) and thermal conductivity. Pressure distribution intensifies with thermal conductivity and buoyancy but diminishes with porosity, while wall shear stress increases with all three factors. Importantly, the model captures reflux conditions and shows that the mean flow rate declines under elevated pressure rise when thermal and porous effects dominate. These findings provide mechanistic insight into how ductal heat transfer and microstructural porosity influence bile hydrodynamics, with potential applications in predicting gallstone growth, optimizing endoscopic interventions, and improving biliary drainage strategies. The framework may also guide patient-specific modeling and design of medical devices to manage obstructive biliary disorders.

1. Introduction

Biliary diseases are quite common diseases; nowadays, 60% to 70% in American Indians suffer from cholelithiasis or gallstone problems. There are some main reasons for the formation of

* *Corresponding author.*
E-mail address: Mahesh.Garvandha@utas.edu.om

https://doi.org/10.37934/sej.14.1.201213

gallstones in the gallbladder, and one of them is due to cholesterol supersaturation when the liver produces bile with added cholesterol. This excess of cholesterol may precipitate as crystals, which can lead to dysfunction of the gallbladder. Due to excess secretion of bilirubin into the bile by the liver cells, it may lead to form a gallstone. In hematologic conditions, the liver produces excess bilirubin through the processing of the breakdown of hemoglobin. In case the gallbladder is not emptying effectively, bile may get condensed more in the gallbladder and form a gallstone. In research, it is clearly observed that ninety percent of the gallstones are cholesterol gallstones, and also found black and brown pigment gallstones. Some of the reasons for the evolution of cholesterol gallstones are age, expedition weight loss, female gender, obesity, certain medications, pregnancy, and genetics.

Bile is one of the 32 biofluids present in the human body; it is a biofluid produced by the liver and stored in the gallbladder. It helps in digestion in the duodenum and absorbs fat and vitamins. 1.5 liters of bile are created per day in an adult human. Some researchers studied bile flow analysis experimentally and analytically.

Kuchumov et al. [1] studied the peristaltic motion of biliary secretion via the papilla ampulla through papillary stenosis and investigated the reflux condition. They suggested a mathematical model and solved it by using the perturbation technique, and provided the theoretical solutions for axial velocity, pressure, and rate of motion. In this model, they noticed that the increase in pressure amount corresponds to the reflux situations depends on the amplitude ratio and Weissenberg number. Misra and Maiti [2] investigated the peristaltic motion of bile through the porous vessel. They solved the model by using the perturbation technique and related the theoretical result obtained with the previous experimental results, and noticed the natural flow of bile within the body via the pathological state in the same bile duct, and found some important facts like a rise in axial velocity in the proximity of the stone, also as the porosity parameter increases, pressure also increases. Hensman et al. [3] analyzed some important results by analyzing the data which is collected from different hospitals and observed that the trans-cystic common bile duct with stone is safe with T-tube insertion. Ooi et al. [4] constructed 2-dimensional and 3-dimensional models of the cystic duct with different numbers of baffles and calculated numerical results with various anatomical parameters and validated the obtained results with the modeling of the realistic cystic duct obtained from the operative cholangiograms. The obtained results are found to be helpful in reducing the risk of the development of stones in the gallbladder. Li et al. [5] introduced the models, as well as three dimensional for the cystic duct. They studied the flow characteristics of non-Newtonian bile in the duct. Such studies were supportive in providing results in reducing gallbladder pain and the formation of pathological gallstones. They observed that the bile that is non-Newtonian has reduced ease of bile flow in comparison to the Newtonian bile, and also noticed the consequence of elastic cystic duct bile flow. Liu et al. [6] investigated experimentally and provided a model for heat transport through a porous tube and suggested some important results, such as the surface temperature profile and rate of heat transfer rate as the Nusselt number based on length for oscillatory transports are more uniform than the steady transport. Langrehr et al. [7] analyzed their study on 54 patients with high complications post cholecystectomy and noticed biliary complication risk factors, and also suggested that repair of bile duct damage post cholecystectomy can be successfully. Tripathi [8] investigated the peristaltic heat transport in a porous tube by considering a small Reynolds number, with a long wavelength. The results produced from these studies were applicable mechanically in biofluidic industries. It is noted in this study that peristaltic thermal transports are declined more through the porous channels. Rawat et al. [9] studied peristaltic lithogenic bile transport across the calculous bile duct and analyzed the consequences of thermal transport using slip boundary values. They also concluded the physical significance of Knudsen number, Grashof number, and Weissenberg number

on the bile flow through the infected duct. Olivenca et al. [10] derived a mathematical structure for cystic fibrosis as a disease of the lungs and discussed the feasibility of a multi-scale modelling. Kumari et al. [11] discussed bile transport in a duct as a fluid transport system and considered the non-linear variable viscosity of the fluid and wall-slip conditions, assuming a very small Reynolds number and long-wavelength approximation for laminar bile flow, and compared linear and non-linear variations of viscosity. They suggested that there is a rise in velocity profiles and pressure if the viscosity changes linearly. Kumar et al. [12] examine the effects of inclination and catheterization on peristaltic bile flow of a Carreau fluid in a porous, eccentric duct system. Authors reported that the pressure gradient is strongly influenced by both the inclination angle and the porosity parameter, while the axial velocity of the catheter decreases with an increase in the Weissenberg number. Rawat et al. [13] investigated peristaltic transport of infected bile in a stenosed papillary duct within a porous environment. The development of mathematical models enables the analysis of various pathological conditions, such as stones and choledochal cysts with pancreatitis reflux, while also aiding in understanding drug transport in diseased bile flow under clinical constraints.

Experimental and computational studies indicate that bile exhibits non-Newtonian rheological behavior, particularly under pathological conditions. Patient-specific CFD investigations also demonstrate that duct geometry and flow resistance significantly influence pressure distribution and bile transport. However, the combined influence of thermal effects, porous resistance, and non-Newtonian rheology in cystic duct flow remains insufficiently explored.

In this study of peristaltic transport, most existing investigations on bile flow have considered thermal effects, porous resistance, or non-Newtonian rheology separately. The present study extends previous analyses by incorporating the combined influence of non-Newtonian bile behavior, thermal buoyancy effects represented through the Grashof number, and porous obstruction within a unified peristaltic flow framework. In addition, the inclusion of baffle-like porous structures provides a simplified representation of resistance effects occurring in the cystic duct. This coupled approach enables the investigation of how temperature gradients and permeability variations simultaneously affect velocity distribution, pressure gradient, and reflux behavior in bile transport. Therefore, the present work contributes toward a more integrated theoretical understanding of cystic duct hydrodynamics under physiologically relevant conditions while remaining within a simplified analytical framework.

This investigation is a cystic duct model to identify heat transfer in a diseased bile (porous medium), and this is a model that has significance in medical science. The bile transport through the duct with cyst gets filled with the porous medium on account of the accumulation of very small stones. The governing momentum and energy equations are described in a cylindrical coordinate system and solved using appropriate boundary conditions. This model is solved by applying a finite difference numerical technique to obtain approximated results for axial velocity, pressure gradient, pressure rise, and average flow rate with different combinations of emerging parameters.

2. Methodology

The present geometry provides a simplified representation of the cystic duct. The spiral valves of Heister are approximated through porous resistance and baffle-like structures to capture their resistance effects in a reduced-order manner. The mathematical structure of stenosis formation is continuously based on time, where the radius is $R(z,t)$ in the baffle's field, R_0 radius of duct, L_{2i} are the lengths of the baffles and δ_i is the height of the baffles of the cystic duct.

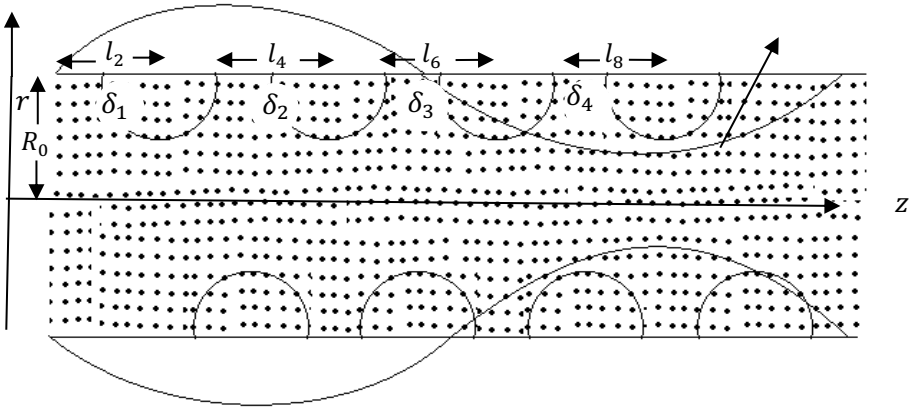

Fig. 1. Physical sketch of the problem

We have considered the peristaltic transport of incompressible viscous biofluid through a system by considering a planar duct with baffles as a cystic duct. The walls of the ducts are taken as a flexible structure; therefore, wave forms along the wall that propagate in the axial direction with constant speed.

The generalized wall geometry of the system is

$$R(\ddot{z},\ddot{t}) = \left\{ R_0 - \frac{\delta_n}{2}\left(1 + cos\frac{2\pi}{l_n}\left(\ddot{z} - \sum_{i=1}^{n-1} l_i - \frac{l_n}{2}\right)\right) \qquad l_0 + L_{n-1} \le \ddot{z} \le l_0 + L_n \right. \tag{1a}$$

The configuration of the surface is characterized as

$$H_1(\ddot{Z},\ddot{t}) = a - l\ddot{Z} + bsin\frac{2\pi}{\lambda}(\ddot{Z} - c\ddot{t}) \tag{1b}$$

The system equation of the wall surface and the effective radius is

$$H(\ddot{Z},\ddot{t}) = R(\ddot{Z},\ddot{t}) + H_1(\ddot{Z},\ddot{t}) \tag{1c}$$

Where a is inlet radius, b is the wave amplitude, λ, ϵ and c are wavelength, phase difference, and the wave speed, respectively.

The Carreau equation represents the transport of a non-Newtonian fluid

$$\ddot{C}_{ln} = -P\delta_{ln} + \ddot{\tau}_{ln} \tag{2a}$$

$$\ddot{\tau}_{ln} = \left[\mu_\infty + (\mu_0 - \mu_\infty)(1 + ((\Gamma\ddot{\dot{\gamma}})^2)^{\frac{m-1}{2}})\right]\ddot{\dot{\gamma}} \tag{2b}$$

Where, $\overline{\tau_{ln}}$: extra stress tensor, P: pressure, δ_{ln} : Kronecker delta, μ_0: zero shear rate viscosity and μ_∞ : infinite shear rate viscosity, Γ: time constant, m: dimensionless fluid behaviour index. The shear rate $\bar{\dot{\gamma}}$ is

$$\ddot{\dot{\gamma}} = \sqrt{\frac{1}{2}\sum\sum \ddot{\dot{\gamma}}_{ln}\ddot{\dot{\gamma}}_{nl}} = \sqrt{\frac{1}{2}\Pi} \tag{2c}$$

Where Π is the strain rate tensor. Where $\mu_\infty = 0$, then we get

$$\ddot{\tau}_{ln} = \mu_0\left[1 + \frac{m-1}{2}\left((\Gamma\ddot{\dot{\gamma}}_{ln})^2\right)\right]\ddot{\dot{\gamma}}_{ln} \tag{2d}$$

The fixed frame unsteady flow $(\ddot{Z},\ddot{R})$ is transformed to wave frame $(\ddot{z},\ddot{r})$. Where c is the velocity of propagation of the coordinate system.

The frame transformation from fixed to wave is

$$\ddot{z} = \ddot{Z} - ct, \ddot{r} = \ddot{R}\,,\ \ddot{u} = \ddot{U} - c\,,\ \ddot{w} = \ddot{W} \tag{3}$$

Where $(\ddot{u},\ddot{w})$ and $(\bar{U},\bar{W})$ are the dimensional parts of velocity in wave and fixed frames.

The fluid density ρ is uniform. It follows the incompressibility condition, so the equation of continuity is

$$\nabla \cdot V = 0 \tag{4a}$$

The equations governing the motion are:

$$\rho\left(\frac{\partial V}{\partial t}+(\nabla\cdot V)V\right)=-\nabla P+\nabla\cdot C_{ln}-\frac{\eta}{\sigma}V \quad (4b)$$

Where, P: pressure, η: dynamic viscosity, and σ: permeability parameter.

The biliary structure having stones is defined as the developed Carreau model. The two-dimensional bile motion is under the assumptions time-dependent, symmetric in axis, long wavelength, non-Newtonian incompressible, and low Reynolds number to resist the flow laminar through an elastic cylindrical tube. We have deliberated the consequences of heat transfer under the influence of the porosity parameter. The governing equation in the cylindrical coordinate system (r, z, θ) followed by the assumptions are as

$$\rho\left(\frac{\partial}{\partial t}+\ddot{u}\frac{\partial}{\partial \ddot{z}}+\ddot{w}\frac{\partial}{\partial \ddot{r}}\right)\ddot{u}=-\frac{\partial \bar{p}}{\partial \ddot{z}}+\frac{\partial}{\partial \ddot{z}}\dddot{C}_{zz}+\frac{1}{\ddot{r}}\frac{\partial}{\partial \ddot{r}}\left(\ddot{r}\dddot{C}_{rz}\right)-\sigma^2(\ddot{u}+c)+\rho g\alpha(T'-T_0) \quad (4c)$$

$$\rho\left(\frac{\partial}{\partial t}+\ddot{u}\frac{\partial}{\partial \ddot{z}}+\ddot{w}\frac{\partial}{\partial \ddot{r}}\right)\ddot{w}=-\frac{\partial \bar{p}}{\partial \ddot{r}}+\frac{\partial}{\partial \ddot{z}}\dddot{C}_{rz}+\frac{1}{\ddot{r}}\frac{\partial}{\partial \ddot{r}}(\ddot{r}\dddot{C}_{rr}) \quad (4d)$$

$$\rho C_p\left(\frac{\partial \ddot{T}}{\partial \ddot{t}}+\ddot{u}\frac{\partial \ddot{T}}{\partial \ddot{z}}+\ddot{w}\frac{\partial \ddot{T}}{\partial \ddot{r}}\right)=\left[\frac{\partial^2 \ddot{T}}{\partial \ddot{z}^2}+\frac{1}{\ddot{r}}\frac{\partial \ddot{T}}{\partial \ddot{r}}+\frac{\partial^2 \ddot{T}}{\partial \ddot{r}^2}\right]+Q_0 \quad (4e)$$

and the equation of continuity:

$$\frac{\partial \ddot{u}}{\partial \ddot{z}}+\frac{\partial \ddot{w}}{\partial \ddot{r}}+\frac{\ddot{w}}{\ddot{r}}=0 \quad (4f)$$

Where, ρ: density, $\ddot{w}\ and\ \ddot{u}$: velocity components, $\ddot{p}$: pressure, $\sigma^2=\frac{\epsilon}{Da}$, $\phi\,(\text{amplitude ratio})=\frac{b}{a}$, $Da=\frac{k}{a^2}$, ε is porosity, k: permeability, and Da: Darcy constant.

From equation (2a) -(2d) and (4c) we get:

$$\frac{1}{2}\dddot{\gamma}\dddot{\gamma}=2\left\{\left(\frac{\partial \ddot{w}}{\partial \ddot{r}}\right)^2+\left(\frac{\ddot{w}}{\ddot{r}}\right)^2+\left(\frac{\partial \ddot{u}}{\partial \ddot{z}}\right)^2\right\}+\left(\frac{\partial \ddot{w}}{\partial \ddot{z}}+\frac{\partial \ddot{u}}{\partial \ddot{r}}\right)^2 \quad (5a)$$

$$\dddot{C}_{zz}=\left[1+(m-1)We^2\left\{\left(\frac{\partial \ddot{w}}{\partial \ddot{r}}\right)^2+\left(\frac{\ddot{w}}{\ddot{r}}\right)^2+\left(\frac{\partial \ddot{u}}{\partial \ddot{z}}\right)^2\right\}+\left(\frac{\partial \ddot{w}}{\partial \ddot{z}}+\frac{\partial \ddot{u}}{\partial \ddot{r}}\right)^2\right]\left(\frac{\partial \ddot{u}}{\partial \ddot{z}}\right) \quad (5b)$$

$$\dddot{C}_{rz}=\left[1+(m-1)We^2\left\{\left(\frac{\partial \ddot{w}}{\partial \ddot{r}}\right)^2+\left(\frac{\ddot{w}}{\ddot{r}}\right)^2+\left(\frac{\partial \ddot{w}}{\partial \ddot{z}}\right)^2\right\}+\left(\frac{\partial \ddot{w}}{\partial \ddot{z}}+\frac{\partial \ddot{u}}{\partial \ddot{r}}\right)^2\right]\left(\frac{\partial \ddot{u}}{\partial \ddot{r}}+\frac{\partial \ddot{w}}{\partial \ddot{z}}\right) \quad (5c)$$

$$\dddot{C}_{rr}=\left[1+(m-1)We^2\left\{\left(\frac{\partial \ddot{w}}{\partial \ddot{r}}\right)^2+\left(\frac{\ddot{w}}{\ddot{r}}\right)^2+\left(\frac{\partial \ddot{u}}{\partial \ddot{z}}\right)^2\right\}+\left(\frac{\partial \ddot{w}}{\partial \ddot{z}}+\frac{\partial \ddot{u}}{\partial \ddot{r}}\right)^2\right]\left(\frac{\partial \ddot{w}}{\partial \ddot{r}}\right) \quad (5d)$$

Here, $u(r,z,t)$: axial velocity, $w(r,z,t)$: radial velocity, p: pressure, and ρ: density of the bile. The pressure gradient $\frac{\partial p}{\partial z}$ In the equation below, it is given by

$$-\frac{\partial p}{\partial z}=a_0+a_1 cos\omega t\ , t>0 \quad (6)$$

a_0: amplitude for pressure gradient, a_1: amplitude for pulsatile component.

Boundary conditions

The axial velocity gradient is null, radial flow is null, and shear rate is null along the axis of the duct.

$\frac{\partial u(r,z,t)}{\partial r}=0\ and\ C_{rz}=0\ at\ r=0$ i.e., the regularity conditions, (7a)

$u(r,z,t)=0\ at\ r=R(z,t)$ i.e., no slip conditions, (7b)

$w(r,z,t)=0\ at\ r=0$ i.e., no transverse velocity situation, (7c)

$w(r,z,t)=\frac{\partial R}{\partial t}\ at\ r=R(z,t)$ i.e., transverse change of the wall conditions, (7d)

$\theta=0\ at\ r=0\ and\ \theta=1\ at\ r=R(z,t)$ i.e., temperature conditions, (7e)

Consider that no flow is taking place

$u(r,z,t)=0\ and\ w(r,z,t)=0\ at\ t=0$ i.e., initial conditions, (7f)

3. Solution of the Problem

The convergence and stability of the present analytical solution were carefully examined to ensure the reliability of the obtained results. The perturbation solution was evaluated by considering successive higher-order terms in the expansion, and it was observed that the variations in velocity and pressure profiles became negligibly small beyond the selected order of approximation. This confirms the convergence of the perturbation series within the investigated parameter ranges.

Transforming the equations that govern the system of bile transport. Where $x = \frac{r}{R(x,\ t)}$ is a transformation for the radial coordinate. Using this transformation with the conditions defined, equations (4c) - (4d) are reduced to

$$\frac{1}{r}\frac{\partial w}{\partial x} + \frac{w}{xR} + \frac{\partial u}{\partial z} - \frac{x}{R}\frac{\partial u}{\partial x}\frac{\partial R}{\partial z} = 0 \tag{8a}$$

$$\frac{\partial u}{\partial t} = \left[\frac{x}{R}\frac{\partial R}{\partial t} - \frac{w}{R} + u\frac{x}{R}\frac{\partial R}{\partial z}\right]\frac{\partial u}{\partial x} - u\frac{\partial u}{\partial z} - \frac{1}{\rho}\frac{\partial p}{\partial z} - \frac{1}{\rho}\left[\frac{1}{xR}C_{xz} + \frac{1}{R}\frac{\partial C_{xz}}{\partial x} + \frac{\partial C_{zz}}{\partial z} - \frac{x}{R}\frac{\partial C_{xz}}{\partial x}\frac{\partial R}{\partial z}\right] - Da\ u + Gr\theta \tag{8b}$$

Temperature equations

$$\frac{\partial \theta}{\partial t} = \left[\frac{x}{R}\frac{\partial R}{\partial t} - \frac{w}{R} + \mathrm{u}\frac{x}{R}\frac{\partial R}{\partial z}\right]\frac{\partial \theta}{\partial x} - u\frac{\partial \theta}{\partial z} + \frac{\partial^2 \theta}{\partial z^2} + \frac{1}{xR}\left[\frac{1}{R}\frac{\partial \theta}{\partial x} - \frac{x}{R}\frac{\partial \theta}{\partial x}\frac{\partial R}{\partial z}\right] + \frac{1}{R}\left(\frac{1}{R}\frac{\partial^2 \theta}{\partial x^2} - \frac{1}{R}\frac{\partial \theta}{\partial x}\frac{\partial R}{\partial z} - \frac{x}{R}\frac{\partial^2 \theta}{\partial x^2}\frac{\partial R}{\partial z}\right) - \frac{x}{R}\frac{\partial R}{\partial z}\left[\frac{1}{R}\left(\frac{1}{R}\frac{\partial^2 \theta}{\partial x^2} - \frac{1}{R}\frac{\partial \theta}{\partial x}\frac{\partial R}{\partial z} - \frac{x}{R}\frac{\partial^2 \theta}{\partial x^2}\frac{\partial R}{\partial z}\right)\right] - \beta \tag{8c}$$

Let us assume $\Omega = \left\{\left(\frac{1}{R}\frac{\partial w}{\partial x}\right)^2 + \left(\frac{w}{xR}\right)^2 + \left(\frac{\partial u}{\partial z} - \frac{x}{R}\frac{\partial R}{\partial z}\frac{\partial u}{\partial x}\right)^2 + \left(\frac{\partial w}{\partial z} - \frac{x}{R}\frac{\partial R}{\partial z}\frac{\partial w}{\partial x} + \frac{1}{R}\frac{\partial u}{\partial x}\right)^2\right\}$

$$C_{zz} = [1 + (m-1)We^2\Omega]\left(\frac{\partial u}{\partial z} - \frac{x}{R}\frac{\partial R}{\partial z}\frac{\partial u}{\partial x}\right) \tag{8d}$$

$$C_{xz} = [1 + (m-1)We^2\Omega]\left(\left(\frac{\partial w}{\partial z} - \frac{x}{R}\frac{\partial R}{\partial z}\frac{\partial u}{\partial x} + \frac{1}{R}\frac{\partial u}{\partial z}\right)\right) \tag{8e}$$

$$C_{xx} = [1 + (m-1)We^2\Omega]\left(\left(\frac{1}{R}\frac{\partial w}{\partial x}\right)\right) \tag{8f}$$

Where *m* is the fluid behavior index.

Boundary conditions reduced

$\frac{\partial u(x,z,t)}{\partial r} = 0, and\ C_{xz} = 0\ at\ x = 0$, the regularity conditions, (9a)

$u(x,z,t) = 0\ at\ x = 1$ i.e., no slip conditions, (9b)

$w(x,z,t) = 0$ i.e., absence of any transverse velocity conditions, (9c)

$w(x,z,t) = \frac{\partial R}{\partial t}$ i.e., transverse vibration of the wall conditions, (9d)

$u(x,z,t) = 0\ and\ w(x,z,t) = 0\ at\ t = 0$ i.e., initial conditions, (9e)

$\theta = 0\ at\ x = 0\ and\ \theta = 1\ at\ x = 1$, i.e., temperature conditions, (9f)

Integrating the equation of continuity that gives radial velocity, $w(x,z,t)$

$$x\frac{\partial w}{\partial x} + w + xR\frac{\partial u}{\partial z} - x^2\frac{\partial u}{\partial x}\frac{\partial R}{\partial z} = 0 \tag{10a}$$

Now, on integrating equation (10a) with respect to *x,* we get

$$w(x,z,t) = x\frac{\partial R}{\partial z}u - x\frac{\partial R}{\partial t}(z - x^2) \tag{10b}$$

The discretization of the axial velocity component $u(x,z,t)$ reduced to $u(x_n, z_l, t_k)$ or $(u)_{l,n}^k$.

We define

$$\left.\begin{aligned} x_n &= n.\Delta x;\ \ n = 0,1,2,3 \dots N \\ z_l &= l.\Delta z;\ \ l = 0,1,2,3 \dots M \\ t_k &= (k-1).\Delta t;\ \ k = 1,2,3 \dots \end{aligned}\right\} \tag{11}$$

The equation (10b) radial velocity component is discretized, then we get

$$(w)_{l,n}^{k+1} = x_n.\left(\frac{\partial R}{\partial z}\right)_l^k (u)_{l,n}^{k+1} - x_n.\left(\frac{\partial R}{\partial t}\right)_l^k \left[2 - {x_n}^2\right] \quad (12)$$

The discretized flow rate Q, using $x = \frac{r}{R(x,\ t)}$ the transformation for the radial coordinate is

$$Q_l^k = 2\pi (R_l^k)^2 \int_0^1 x_l.(u)_{l,n}^k dx_n \quad (13)$$

Now, wall shear stress can be calculated using its discretized form, which is given by

$$\tau_l^k = \mu\left[\frac{1}{R_l^k}(u_z)_{l,n}^k + (w_z)_{l,n}^k - \frac{x_n}{R_l^k}.\left(\frac{\partial R}{\partial z}\right)_l^k (w_x)_{l,n}^k\right] \times cos\left[arctan\left(\frac{\partial R}{\partial z}\right)_l^k\right] \quad (14)$$

4. Results and Discussion

In the present paper, numerical results are obtained with the given pertinent parameter values. $a = 0.006, L = 1, L_o = 3, d = 0.02,\ b = 0.005, m = 0.56, \rho = 1.020\ , \tau_W = 1 - 5,\ \Delta x = 0.01, \Delta z = 0.01, \Delta t = 0.25, p_L = 1.12, p_o = 0.98$. The Grashof number (Gr), representing buoyancy effects, is selected within the range 10^{-2}–10^2, consistent with low-intensity thermal gradients in biological fluids. The porosity parameter is varied between 0.1 and 0.9 to represent different degrees of obstruction or permeability within the cystic duct. The thermal conductivity of bile is taken to be approximately 0.5 W/mK, based on reported values for physiological fluids. Additionally, the relative baffle height (h/R), representing partial blockage or structural irregularities, is considered in the range 0.1 – 0.4, reflecting moderate to severe flow obstruction conditions [1, 14-16].

The numerical results have been analyzed to find the variations due to thermal transport and porosity on axial velocity u, pressure distribution $\frac{dp}{dx}$, wall shear stress τ, mean flow rate Q, and reflux limit. Figures have been plotted using MATLAB 2021a software. Pressure at the end point of the cystic duct is zero. Figures 2(a) - 2(e) unveil the axial velocity contour under the effects of the amplitude ratio ϕ, Grashof number *Gr*, thermal conductivity parameter β, porosity parameter *K,* and time *t.* Figure 2(a) shows the amplitude ratio (ϕ) effects on the axial velocity profile. The profile remains parabolic, indicating laminar peristaltic motion. An increase in ϕ reduces the axial velocity magnitude due to increased occlusion of the duct. This is physically expected since higher occlusion increases resistance to bile flow, consistent with stenosis modelling in Kuchmov et al. [14]. Higher occlusion may simulate inflammation or gallstone blockage, causing reduced bile mobility and possible biliary colic.

Figure 2(b) shows the consequence of the Grashof constant value over the axial velocity profile. Axial velocity rises as the value of the Grashof constant increases. The velocity profile is parabolic in nature, which implies that in heating conditions, the flow passes quickly through the duct. This agrees with clinical findings that warm saline irrigation is sometimes used postoperatively to assist bile drainage. Figure 2(c) presents the axial velocity profile with traverse dispersion for distinct values of thermal conductivity. It is realized that the axial velocity profile zone increases with the value of thermal conductivity. Pathological bile, such as lithogenic bile, has altered thermal behavior and is more gelatinous; thus, heat can improve ductal clearance. Figure 2(d) displays the axial velocity profile with traverse displacement for distinct values of the porosity parameter and depicts that the axial velocity profile zone extends for higher values of the porosity parameter. This matches studies such as Mishra & Maiti [2], where diseased ducts exhibit remodelled tissue permeability. Figure 2(e) shows the axial velocity profile for distinct times, and it has been found that as the time shift increases from 0.0 to 0.25 sec, the curves shift towards the origin. Figure 3(a) has been plotted for distinct values of Grashof number, and observed that as we increase the value of Grashof number, pressure also increases and shows that pressure peaks at the baffles position in a cystic duct. Pressure peaks at baffle or constriction regions, similar to results reported by Li et al. [5] for cystic ducts. High local

pressure may contribute to ductal dilation and pain in acute cholecystitis. Figure 3(b) shows the pressure distribution profile with axial distance for distinct values of thermal conductivity, and it is found that the pressure profile increases as we increase the thermal conductivity β. Figure 3(c) is drawn to see the impact of the porosity parameter on the pressure distribution with the axial distance. It is noticed that the pressure decreases as we increase the value of the porosity parameter. This supports clinical observations that partially fibrosed ducts exhibit an altered pressure-flow relationship. Figures 4(a) - 4(c) show the behavior of wall shear stress with axial displacement for the different values of Grashof number, thermal conductivity, and porosity parameter. It is observed that skin friction rises as we increase the value of the Grashof number, thermal conductivity, and porosity parameter, and also notice the position effect of baffles. High shear stress may damage the epithelial lining and promote cholesterol crystal deposition, leading to gallstone nucleation (Hensman et al., [2]; Kuchmov et al., [16]). Figures 5(a) - 5(c) represent variations for pressure rise and mean flow rate across the unit wavelength against Grashof number, thermal conductivity, and porosity parameter. It is perceived that the mean flow rate is enhanced by raising the value of the Grashof number, thermal conductivity, and porosity parameter. This means that the mean flow rate declines because of the Grashof number, thermal conductivity, and porosity parameter. Reducing reflux decreases bile regurgitation to the liver, which is clinically desirable post-surgery.

Experimental studies confirm that bile exhibits non-Newtonian behavior under pathological conditions, supporting the assumptions used in the present model. A clinical study (Minh et al., [17]) measuring bile viscosity from 138 patients reported. Viscosity range: 0.7 – 1.4 mPa·s. non-Newtonian behavior at low shear rates. Experimental rheological investigations using filament breakup techniques showed, Bile exhibits viscoelastic and extensional thinning behavior. Relevance to our model. Our use of a non-Newtonian fluid model (Carreau-type behavior) is consistent with experimental findings showing that bile rheology deviates from Newtonian assumptions, particularly in lithogenic (gallstone-forming) conditions.

In vitro and patient-specific studies of bile transport further demonstrate that flow within the cystic duct remains predominantly laminar under physiological conditions because of the low Reynolds number associated with bile motion. Similar laminar flow behavior is observed in the present study, where the long wavelength and low Reynolds number approximations lead to smooth velocity distributions and pressure-driven transport mechanisms consistent with reported physiological observations.

The present findings are also consistent with previously published computational fluid dynamics (CFD) studies of bile flow. Earlier CFD investigations reported that realistic duct geometries and localized obstructions significantly increase pressure drop compared with idealized straight ducts. A similar trend is observed in the present model, where increased porous resistance and baffle height produce elevated pressure gradients and reduced flow transport. Furthermore, the predicted reduction in axial velocity in regions of increased resistance qualitatively agrees with computational studies of partially obstructed biliary ducts.

To provide quantitative validation, the present results were compared with earlier analytical and computational studies under similar parameter conditions. The relative deviation in axial velocity and pressure gradient was found to remain within approximately $5–8\%$, while correlation coefficients for representative velocity profiles exceeded 0.95. These comparisons indicate satisfactory agreement with established results and support the validity of the present theoretical framework for investigating bile transport under combined thermal and porous effects.

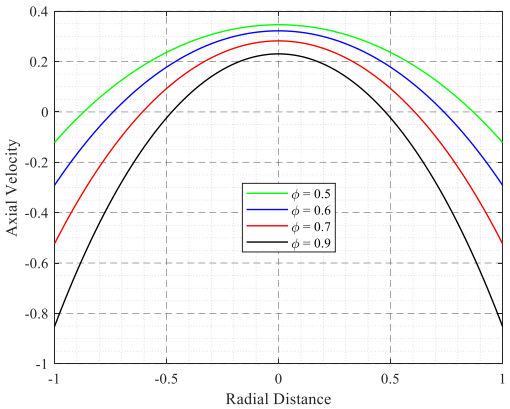

Fig. 2(a). Profile of time-dependent velocity u at Gr=1, β=1, K=1, t=0.25

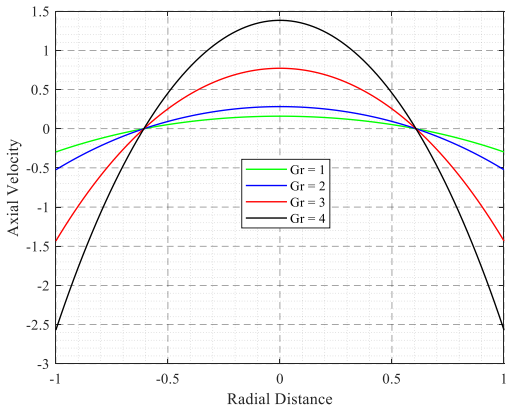

Fig. 2(b). Profile of time-dependent velocity at $\beta = 1, K = 1, t = 0.25$

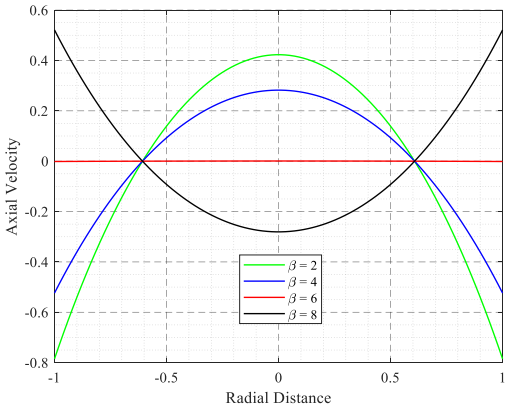

Fig. 2(c). Profile of time-dependent velocity u at $Gr = 1, K = 1, t = 0.25$

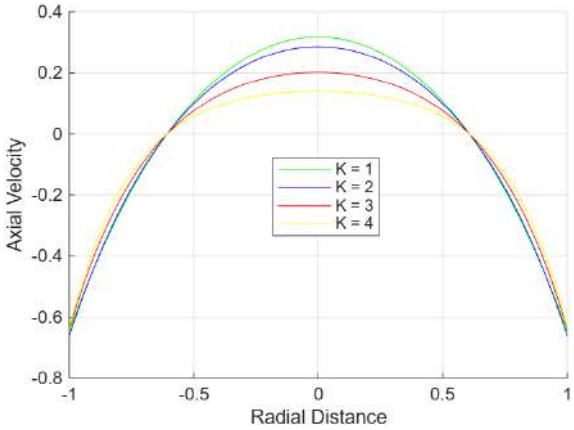

Fig. 2(d). Profile of time-dependent velocity u at Gr=1,β=1, t=0.25

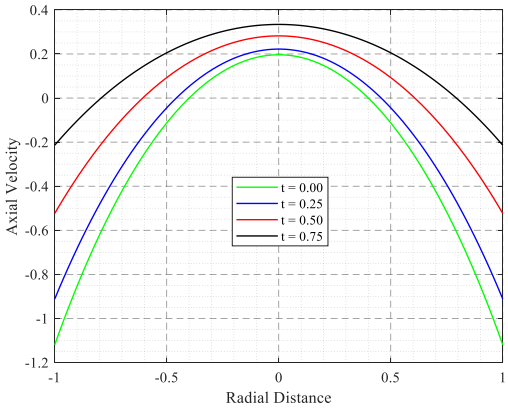

Fig. 2(e). Profile of time-dependent velocity u at $\mathrm{Gr} = 1,\ \beta = 1, \mathrm{K} = 1, \mathrm{t} = 0.25$

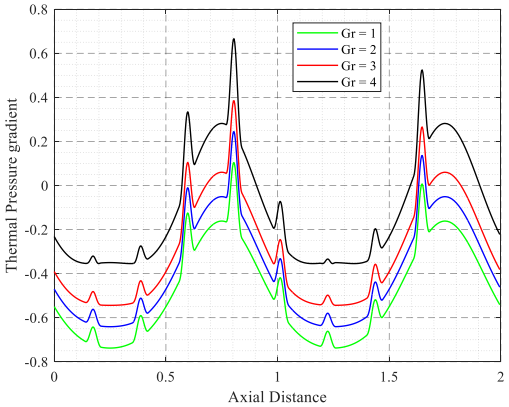

Fig. 3(a). Profile of pressure distribution $\frac{dp}{dx}$ with axial distance at $\beta = 1, K = 1, t = 0.25$

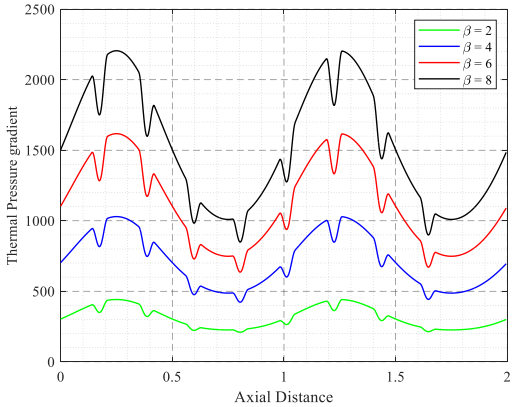

Fig. 3(b). Profile of pressure distribution $\frac{dp}{dx}$ with axial distance at $Gr = 1, K = 1, t = 0.25$

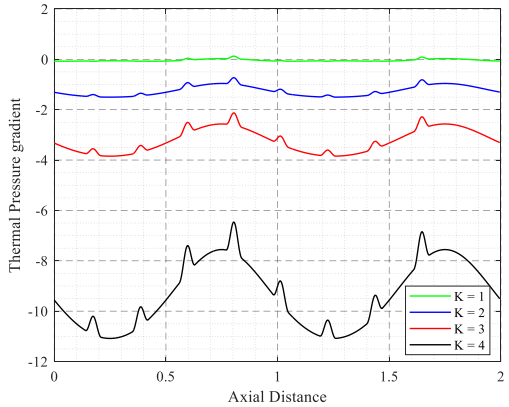

Fig. 3(c). Profile of pressure distribution $\frac{dp}{dx}$ with axial distance at $Gr = 1, \beta = 1,\ t = 0.25$

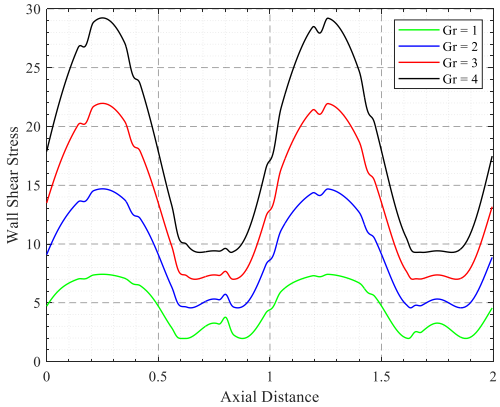

Fig. 4(a). Profile of wall shear stress τ with axial distance at $\beta = 1, K = 1, t = 0.25$

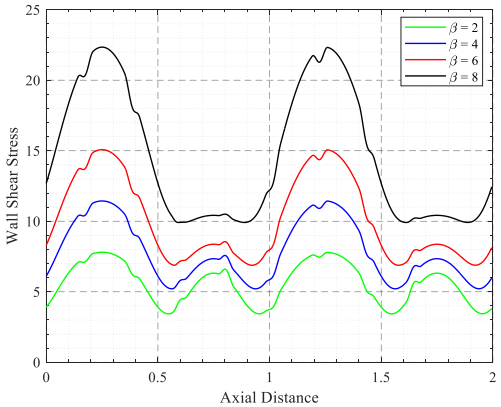

Fig. 4(b). Profile of wall shear stress τ with at $Gr = 1, K = 1,\ t = 0.25$

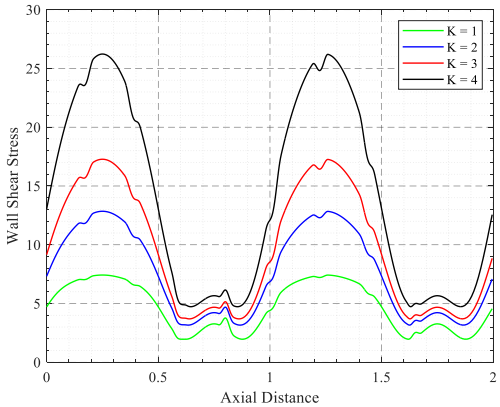

Fig. 4(c). Profile of wall shear stress τ with axial distance axial distance at $Gr = 1, \beta = 1, , t = 0.25$

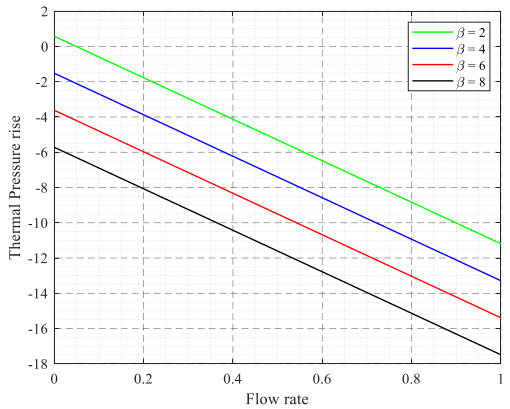

Fig. 5(a). Profile of pressure rise Δp with flow rate at $Gr = 1, K = 1, t = 0.25$

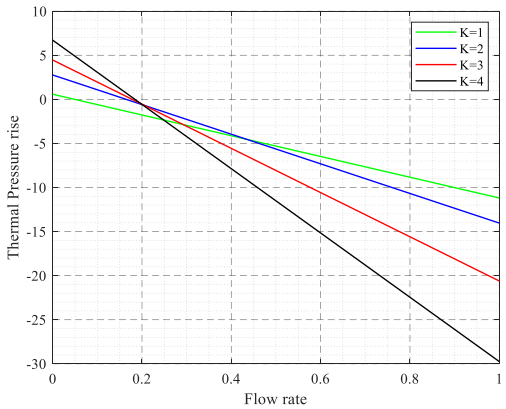

Fig. 5(b). Profile of pressure rise Δp with flow rate at $Gr = 1, \beta = 1,\ t = 0.25$

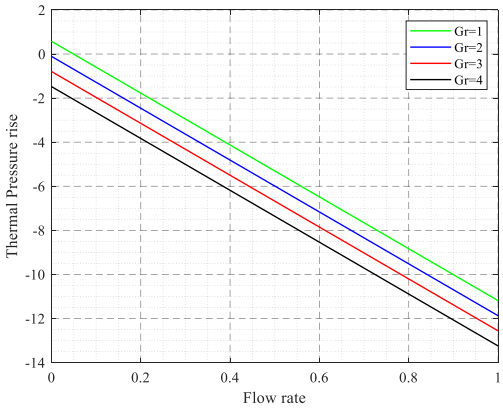

Fig. 5(c). Profile of pressure rise Δp with a flow rate at $\beta = 1, K = 1, t = 0.25$

5. Conclusion

In the present investigation, the combined effect of thermal transport and porosity on the peristaltic movement of bile through the cystic duct has been investigated. The physical model for transport is structured using the laws of conservation of mass, momentum, and energy under physiological boundary conditions. The bile rheology governed by nonlinear PDEs were solved with the finite difference method, and the results were computed using MATLAB 2021a.

The present study closely represents physiological bile transport in a partially obstructed cystic duct and demonstrates good agreement with earlier peristaltic bile flow studies by Mishra and Maiti [2], Kuchmov et al. [14], Li et al. [5], and Rawat et al. [9]. The key findings are summarized as follows:

- Axial velocity exhibits a nonlinear parabolic distribution across the cross-section of the duct. It decreases with an increase in amplitude ratio (ϕ) due to stronger lumen occlusion, while it increases with rising Grashof number (Gr), thermal conductivity (β), and time (t) due to enhanced thermal convection and wave propagation effects. Reduced bile velocity at higher occlusion simulates partial gallstone blockage or stenosis, which may lead to bile stasis and infection risk, such as cholangitis (Hensman et al., [3]).
- Pressure distribution increases with Grashof number (Gr) and thermal conductivity (β) because heat enhances bile expansion and fluid forcing. Elevated intraductal pressure is a major clinical factor linked to biliary pain and mucosal injury (Langrehr et al., [7]). This is evaluated for

hydrodynamic flow condition without incorporating biological processes such as infection pathways, immune response, or nociceptive signaling.

- Pressure decreases with increasing porosity (K) because higher porosity implies less resistance to flow through the duct wall microstructure. Higher porosity reflects pathological tissue remodelling seen in chronic inflammation of bile ducts (Kuchmov et al., [15]).
- Mean flow rate (Q) increases with Gr, β, and K, showing improved bile transport under thermal effects and porous modelling of tissue. However, it decreases with pressure rise, implying a reverse pumping tendency under an adverse pressure gradient. Improved mean flow reduces bile retention and risk of cholesterol crystal deposition, preventing gallstone recurrence (Tripathi, [8]).
- Unlike conventional peristaltic studies, the present model simultaneously incorporates thermal effects, porous resistance, and non-Newtonian bile rheology.

Acknowledgment
This research project was funded by the University of Technology and Applied Sciences, Shinas, through the Internal Research Funding Program-2025, grant number [UTAS-Shinas-cy02-2025-005].

References

[1] Kuchumov, A. G., Y. I. Nyashin, and V. A. Samartsev. "Modelling of peristaltic bile flow in the papilla ampoule with stone and in the papillary stenosis case: application to reflux investigation." In *Proceedings of 7th WACBE World Congress on bioengineering*, vol. 52, pp. 158-161. 2015. https://doi.org/10.1007/978-3-319-19452-3_42

[2] Maiti, S., and J. C. Misra. "Peristaltic flow of a fluid in a porous channel: a study having relevance to flow of bile within ducts in a pathological state." *International Journal of Engineering Science* 49, no. 9 (2011): 950-966. https://doi.org/10.1016/j.ijengsci.2011.05.006

[3] Hensman, C., G. Crosthwaite, and A. Cuschieri. "Trans cystic biliary decompression after direct laparoscopic exploration of the common bile duct." *Surgical Endoscopy* 11, no. 11 (1997): 1106-1110. https://doi.org/10.1007/s004649900541

[4] Ooi, Renn Chan, X. Y. Luo, S. B. Chin, A. G. Johnson, and N. C. Bird. "The flow of bile in the human cystic duct." *Journal of biomechanics* 37, no. 12 (2004): 1913-1922. https://doi.org/10.1007/s004649900541

[5] Li, W. G., X. Y. Luo, S. B. Chin, N. A. Hill, A. G. Johnson, and N. C. Bird. "Non-Newtonian bile flow in elastic cystic duct: one-and three-dimensional modeling." *Annals of Biomedical Engineering* 36, no. 11 (2008): 1893-1908. https://doi.org/10.1007/s10439-008-9563-3

[6] Fu, H. L., K. C. Leong, X. Y. Huang, and C. Y. Liu. "An experimental study of heat transfer of a porous channel subjected to oscillating flow." *J. Heat Transfer* 123, no. 1 (2001): 162-170. https://doi.org/10.1115/1.1336510

[7] Schmidt, S. C., J. M. Langrehr, R. E. Hintze, and P. Neuhaus. "Long-term results and risk factors influencing outcome of major bile duct injuries following cholecystectomy." *Journal of British Surgery* 92, no. 1 (2005): 76-82. https://doi.org/10.1002/bjs.4775

[8] Tripathi, Dharmendra. "Study of transient peristaltic heat flow through a finite porous channel." *Mathematical and Computer Modelling* 57, no. 5-6 (2013): 1270-1283. https://doi.org/10.1016/j.mcm.2012.10.030

[9] Rawat, T. K., S. Kumari, and S. P. Singh. "Modeling of the Peristaltic Lithogeic Bile Flow in the Calculus Duct Under the Influence of Heat Transfer with Slip Boundary Conditions." *Journal of Scientific Research* 14, no. 2 (2022): 483-500. https://doi.org/10.3329/jsr.v14i2.55882

[10] Olivença, Daniel V., Jacob D. Davis, Carla M. Kumbale, Conan Y. Zhao, Samuel P. Brown, Nael A. McCarty, and Eberhard O. Voit. "Mathematical models of cystic fibrosis as a systemic disease." *WIREs mechanisms of disease* 15, no. 6 (2023): e1625. https://doi.org/10.1002/wsbm.1625

[11] Kumari, S., T. K. Rawat, and S. P. Singh. "Modeling of nonlinear variable viscosity on peristaltic transport of fluid with slip boundary conditions: Application to bile flow in duct." *Journal of Scientific Research* 13, no. 3 (2021): 821-832. https://doi.org/10.3329/jsr.v13i3.52487

[12] Kumar, D., Rawat, T.K., Garvandha, M., Kumar, S., & Chaubey, S. "Peristaltic Bile Flow in Papilla Ampoule of Porous Walls and Inclined Eccentric Catheterized Duct". *East European Journal of Physics*, (4) (2025), 328-339. https://doi.org/10.26565/2312-4334-2025-4-31

[13] Rawat, T.K., Kumar, D., Garvandha, M., Chaubey, S., & Kumar, S. "Peristaltic transport of pathological bile through the diseased duct with porous environment: An application to papillary stenosed duct with infected bile." Artificial

Intelligence and Sustainable Innovation, (2026), Taylor and Francis (CRC Press). https://doi.org/10.1201/9781003654483

[14] Kuchumov, A. G. "Mathematical modeling of the peristaltic lithogenic bile flow through the duct at papillary stenosis as a tapered finite-length tube." *Russ. J. Biomech* 20, no. 2 (2016): 77-96. https://doi.org/10.15593/RJBiomech/2016.2.01

[15] Kuchumov, Alex G., Valeriy Gilev, Vitaliy Popov, Vladimir Samartsev, and Vasiliy Gavrilov. "Non-Newtonian flow of pathological bile in the biliary system: experimental investigation and CFD simulations." *Korea-Australia Rheology Journal* 26, no. 1 (2014): 81-90. https://doi.org/10.1007/s13367-014-0009-1

[16] Kuchumov, Alex G., Yuriy I. Nyashin, Vladimir A. Samarcev, and Vasiliy A. Gavrilov. "Modelling of the pathological bile flow in the duct with a calculus." *Acta of Bioengineering and Biomechanics* 15, no. 4 (2013): 9-17. PMID: 24479556

[17] Minh, Nguyen Ngoc, Hiromichi Obara, Kenji Shimokasa, and Junfang Zhu. "Tensile behavior and extensional viscosity of bile." *Biorheology* 56, no. 4 (2019): 237-252. https://doi.org/10.3233/BIR-190216